Journal of Photochemistry & Photobiology, B: Biology 234 (2022) 112512

Contents lists available at ScienceDirect

Journal of Photochemistry & Photobiology, B: Biology

journal homepage: www.elsevier.com/locate/jphotobiol

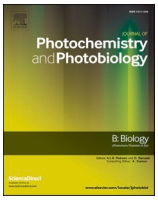

A highly photostable and versatile two-photon fluorescent probe for the detection of a wide range of intracellular nitric oxide concentrations in macrophages and endothelial cells

Carla Arnau del Valle [a], Lewis Williams [a], Paul Thomas [b], Robert Johnson [c], Sathuwarman Raveenthiraraj [c], Derek Warren [c], Anastasia Sobolewski [c], María Paz Muñoz [a], Francisco Galindo [d], María J. Marín [a,*]

[a] School of Chemistry, University of East Anglia, Norwich Research Park, Norwich NR4 7TJ, UK
[b] Faculty of Sciences, University of East Anglia, Norwich Research Park, Norwich NR4 7TJ, UK
[c] School of Pharmacy, University of East Anglia, Norwich Research Park, Norwich NR4 7TJ, UK
[d] Departamento de Química Inorgánica y Orgánica, Universitat Jaume I, Av. Sos Baynat s/n, Castellón de la Plana 12071, Spain

ARTICLE INFO

Keywords:
Near-infrared
Two-photon microscopy
Nitric oxide detection
Macrophages cells
Endothelial cells

ABSTRACT

Nitric oxide (NO) is involved in many biological processes affecting the cardiovascular, nervous and immune systems. Intracellular NO can be monitored using fluorescent probes in combination with fluorescence imaging techniques. Most of the currently available NO fluorescent molecular probes are excited *via* one-photon excitation using UV or Vis light, which results in poor penetration and high photodamage to living tissues. Here, we report a two-photon fluorescent molecular probe, **DANPY-NO**, able to detect NO in live cells. The probe consists of an *o*-phenylenediamine linked to a naphthalimide core; and operates *via* photoinduced electron transfer. **DANPY-NO** exhibits good sensitivity (LOD of 77.8 nM) and high selectivity towards NO, and is stable over a broad range of pHs. The probe targeted acidic organelles within macrophages and endothelial cells, and demonstrated enhanced photostability over a commercially available NO probe. **DANPY-NO** was used to selectively detect endogenous NO in RAW264.7ϒ NO^- macrophages, THP-1 human leukemic cells, primary mouse (bone marrow-derived) macrophages and endothelial cells. The probe was also able to detect exogenous NO in endothelial cells and distinguish between increasing concentrations of NO. The NO detection was evidenced using confocal laser scanning and two-photon microscopies, and flow cytometry. Further evidence was obtained by recording the changes in the intracellular fluorescence emission spectrum of the probe. Importantly, the probe displayed negligible toxicity to the analysed biological samples. The excellent sensitivity, selectivity, stability and versatility of **DANPY-NO** confirm its potential for *in vitro* and *in vivo* imaging of NO.

1. Introduction

Nitric oxide (NO) is a short-lived gaseous free radical involved in many physiological processes of the cardiovascular, nervous and immune systems [1,2]. In mammalian cells, NO is synthesised from L-arginine by nitric oxide synthase (NOS) enzymes including neuronal NOS (nNOS), inducible NOS (iNOS) and endothelial NOS (eNOS) [3,4]. These enzymes are responsible for the endogenous biosynthesis of NO, and differ in structure, function and localization [5]. nNOS and eNOS are calcium-dependent and produce low concentrations of NO (nanomolar) for short periods of time; in contrast, iNOS is calcium-independent and induces a continuous production of NO [6]. NO generated by nNOS in the brain functions as neuromediator and neurotransmitter, having roles in smooth muscle control, behaviour,

Abbreviations: NOS, nitric oxide synthase; iNOS, inducible nitric oxide synthase; eNOS, endothelial nitric oxide synthase; nNOS, neuronal nitric oxide synthase; IFN-ϒ, interferon-gamma; LSM, laser scanning microscopy; PET, photoinduced electron transfer; NIR, near-infrared; L-Arg, L-arginine; AA, ascorbic acid; DHA, dehydroascorbic acid; LOD, limit of detection; LPS, lipopolysaccharide; DIC, differential interference contrast; DMEM, Dulbecco's Modified Eagle Medium; L-NAME, N-nitroarginine methyl ester; DAF-2 DA, 4,5-diaminofluorescein diacetate; BMDMs, bone marrow-derived macrophages; PMA, phorbol 12-myristate 13-acetate; SNAP, *S*-nitroso-*N*-acetylpenicillamine.

* Corresponding author.
E-mail address: m.marin-altaba@uea.ac.uk (M.J. Marín).

https://doi.org/10.1016/j.jphotobiol.2022.112512
Received 27 April 2022; Received in revised form 20 June 2022; Accepted 2 July 2022
Available online 8 July 2022

memory, and being involved in a number of neurodegenerative diseases including Alzheimer's, Huntington's and Parkinson's diseases [7–9]. NO produced by eNOS in endothelial cells of blood vessels functions as a vasodilator regulating functions such as blood flow and pressure, and it is responsible for the inhibition of platelets aggregation and adhesion to the vascular wall [10]. In addition, a decrease in NO levels in plasma is an indication of endothelial dysfunction [11], which further indicates that monitoring NO concentration in plasma could be critical for the diagnosis of cardiovascular diseases. The third form of NOS, iNOS, is involved in immunity and inflammation processes acting both as an inflammatory and anti-inflammatory agent, depending on its concentration and target cell type. iNOS plays important roles in macrophage cell activation and in the destruction of infectious agents [2,12]. iNOS produces large quantities of NO upon stimulation of cells with pro-inflammatory cytokines, such as interferon-gamma (IFN-ϒ) [13]. iNOS is also activated in macrophages following phagocytosis of infection agents to produce high concentrations of NO that will contribute to the destruction of the pathogen. Interestingly, NO has been shown to have a double effect in cancer, being involved in tumour-promotion and tumour-suppression effects which mainly depend on its concentration [5,14], with the cytotoxic effect of NO being exploited in the treatment of cancer [15–17].

Due to the significant role that NO plays in human physiology and disease, research aiming to improve the intracellular monitoring of this free radical has seen an exponential increase in the past decades. Different approaches are being used to detect NO including fluorescence-based bioimaging, spectroscopic analysis, electrochemistry, electron spin resonance spectroscopy, chemiluminescence, or colourimetry [18–21]. Despite the advances reported to date, the direct detection of NO has proven challenging due to its low concentration, short lifetime, and high reactivity with several reactive oxygen species (ROS) [6]. The use of fluorescent molecular probes in conjunction with microscopic techniques such as confocal laser scanning microscopy (LSM) has shown advantages over other techniques for the detection of intracellular NO. These advantages include spatial and temporal resolution and high sensitivity [19,22]. Consequently, considerable efforts have been made to further the availability and applicability of these fluorescent NO molecular probes, being aromatic *ortho*-diamino (*o*-diamino)-fluorophore derivatives the most popular organic fluorescent probes reported for the detection of intracellular NO [23–27].

Despite the large number of fluorescent NO molecular probes reported in the literature for the detection of NO in living biological systems [28–34], there are still limitations that need to be overcome such as the excitation wavelength required for the measurement (mainly UV–Vis) and the high photobleaching which, in turn, affects the sensitivity of the detection and the spatiotemporal resolution. Near-infrared (NIR) excitation overcomes some of the drawbacks of the UV–Vis light as it allows for deeper penetration of biological tissues, and causes minimal photodamage upon long-term irradiation. In addition, the lower-energy excitation using NIR leads to negligible autofluorescence and higher photostability of the probe [35]. Two-photon microscopy employs two NIR photons as the excitation source exhibiting advantages over one-photon microscopy [36].

Several examples of two-photon excitable NO molecular probes have been reported in the literature, most of them based on an aromatic *o*-diamino-fluorophore. For example, Kim and co-workers developed *o*-phenylenediamine-based two-photon fluorescent probes that were able to selectively detect endogenous NO produced by RAW264.7 macrophages and had potential for deep-tissue imaging of NO [37,38]. Further improvements in the ability to monitor NO deep inside tissue were achieved when using a far-red emissive two-photon fluorescent probe based on Nile Red, that permitted the *in situ* tracking of NO in an inflammatory process [39]. Among other two-photon fluorophores, 1,8-naphthalimide has been previously used for the construction of *o*-phenylenediamine-based fluorescent probes for the detection of NO in solution [40,41] and in different biological environments [42–45]. For example, Lyso-NINO was reported as a selective and highly sensitive NO probe that was able to detect endogenous NO in RAW264.7 macrophages and exogenous NO released by a donor in MCF-7 breast cancer cells [42], with low cytotoxicity to the latest. Similarly, the selective and highly sensitive probe for NO, LyNP-NO, was able to detect NO produced exogenously and endogenously in C6 glial cells and endogenously in rat hippocampus [44]. Despite the advances in the development of two-photon NO probes in recent years, to the best of our knowledge, there are no examples in the literature of highly biocompatible fluorescent NO probes that can be used for the successful detection of NO produced by the different forms of NOS in a broad range of biological environments and using different analytical techniques.

Here, we present a highly photostable, selective and biocompatible two-photon fluorescent probe (**DANPY-NO,** Fig. 1) that can be used for the detection of NO produced by iNOS in different macrophages, including a mouse macrophage cell line, primary mouse macrophages and human leukemic cells, and by eNOS in endothelial cells. **DANPY-NO** is a photoinduced electron transfer (PET)-based NO probe consisting of *o*-phenylenediamine linked to a naphthalimide core and bearing a simple piperazine scaffold. **DANPY-NO** shows good sensitivity and excellent selectivity towards NO in solution, and its fluorescence stability at different, biologically-relevant, pH values confirms its suitable applicability in physiological environments. The NO probe furthermore exhibits good photostability as confirmed when compared to a commercially available NO probe, 4,5-diaminofluorescein diacetate (DAF-2 DA), excellent biocompatibility, and extended applicability in cellular environments. The versatility of **DANPY-NO** as NO probe was confirmed using confocal LSM (images and intracellular fluorescence emission spectra), multiphoton microscopy and flow cytometry.

2. Results and Discussion

The novel two-photon NO molecular probe, **DANPY-NO** (Fig. 1), was designed as a PET-based fluorescent probe consisting of a 1,8-naphthalimide two-photon fluorophore conjugated to an *o*-phenylenediamine unit and a carbonyl-piperazine fragment. The NIR-excitable fluorophore, 1,8-naphthalimide, was chosen due to its well-known, remarkable photophysical properties such as good photostability, high quantum yield and pH insensitivity. The piperazine moiety was incorporated due to its versatile structure that could serve as scaffold to further the biological potential of **DANPY-NO**. An acetyl-derivative was specifically chosen here to prevent the protonation of the piperazine fragment at biological pHs. In **DANPY-NO**, the fluorescence emission is

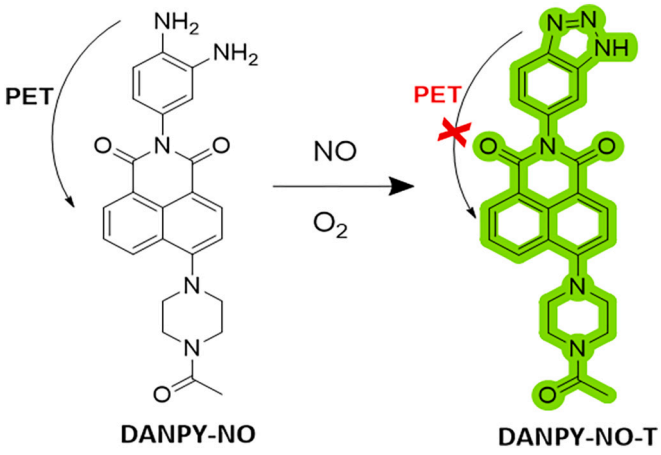

Fig. 1. Chemical structure of the two-photon NO molecular probe (**DANPY-NO**) and its reaction with NO in the presence of oxygen forming the triazole derivative (**DANPY-NO-T**). The fluorescence of the naphthalimide core is quenched in **DANPY-NO** due to a PET process. The formation of **DANPY-NO-T** hinders the PET process restoring the fluorescence of the core.

quenched due to the PET that occurs from the electron-donating *o*-phenylenediamine to the naphthalimide core. The *o*-phenylenediamine moiety reacts with NO, in the presence of oxygen, forming the electron-poor triazole derivative, **DANPY-NO-T**, and enhancing the fluorescence emission of the naphthalimide core. Other examples of PET-based sensors have been reported in the literature for the detection of, for example, pH [46–48], endogenous NADH [49] and singlet oxygen [50], among others.

2.1. Synthesis and Characterisation of *DANPY-NO*

The probe was successfully synthesised in three steps from 4-bromo-1,8-naphthalic anhydride and 2-nitro-*p*-phenylenediamine (**Scheme S1**). **DANPY-NO** and the two intermediates of the synthesis were characterised by ^{1}H NMR, ^{13}C NMR, infrared spectroscopy and high-resolution mass spectrometry (HRMS) (see **Figs. S1–S6** and Materials and Methods section in the SI for detailed characterisation).

The photophysical properties of the NO probe were studied by measuring its UV–Vis absorption, and fluorescence excitation, emission and quantum yield. **DANPY-NO** exhibited a maximum absorption band at 396 nm ($\varepsilon = 1.13{\cdot}10^{4}$ $M^{-1}{\cdot}cm^{-1}$ in DMSO, **Figs. S7a** and **S8**) and a fluorescence emission peak centered at 535 nm in DMSO (**Fig. S7c**), both characteristic of 1,8-naphthalimide structures.

2.2. Sensitivity and Selectivity of *DANPY-NO* towards NO

The ability of **DANPY-NO** to detect NO was first evaluated and confirmed in aqueous solution. As observed in Fig. 2, the weak fluorescence emission intensity of **DANPY-NO** at 556 nm in aqueous solution (13% DMSO) increased by 647% upon addition of an excess of the NO donor diethylamine NONOate (0.5 mM) confirming the ability of the NO probe to detect NO *via* formation of the corresponding triazole, **DANPY-NO-T**. Additionally, a remarkable 13-fold increase in the QY of **DANPY-NO** was observed, in acetonitrile, following addition of NO (*ie.* upon formation of **DANPY-NO-T**). To further confirm the formation of **DANPY-NO-T** upon reaction of **DANPY-NO** with NO in the presence of oxygen, the product of the reaction was isolated and characterised by ^{1}H NMR, and UV–Vis and fluorescence spectroscopies (see **Fig. S9** and **Table S1**). As expected, the ^{1}H NMR peaks corresponding to the aromatic protons on the 1,2-phenylenediamine unit shifted to higher frequencies following the formation of the **DANPY-NO-T** as the sensing mechanism for NO detection.

DANPY-NO exhibited good sensitivity towards NO in aqueous media, with a limit of detection of 77.8 nM (LOD = 3σ/k, σ being the standard deviation of the blank signals and k the slope of the calibration curve, **Fig. S10**). A good linear correlation was obtained between the fluorescence intensity and the NO concentration (from 0 to 30 μM) with a calibration curve measured in triplicate. This low LOD suggests the potential of **DANPY-NO** to be used for the detection of NO produced by different cell lines including macrophages.

The selectivity of **DANPY-NO** towards NO over other potential biological interferences including changes in pH was investigated. The stability of the fluorescence emission intensity of **DANPY-NO** was monitored at pH values of biological relevance showing a pH-insensitive fluorescence response from pH 5 to 9.5 (**Fig. S11**). The pK_a of the probe was calculated to be 3.99 ± 0.14. Additionally, **DANPY-NO** was able to detect the presence of NO both at neutral pHs and at acidic ones (pH *ca.* 4) demonstrating its potential to detect NO also within acidic environments (**Fig. S12**). To investigate the specificity of **DANPY-NO** towards NO, its reactivity with several possible cellular interferences (100 μM), including H_2O_2, NO_2^-, NO_3^-, O_2^-, •OH, $^{1}O_2$, Na^+, K^+, Ca^{2+}, L-arginine (L-Arg), ascorbic acid (AA), dehydroascorbic acid (DHA) and ClO^-, was monitored (Fig. 3). A considerable increase in the fluorescence emission intensity of **DANPY-NO** was only observed following addition of NO, confirming the excellent selectivity of the developed compound towards NO. Furthermore, **DANPY-NO** remained sensitive to NO in the presence of the different species tested (**Fig. S13**). These results further confirm the suitability of **DANPY-NO** for the detection of intracellular NO.

2.3. Characterisation of *DANPY-NO* in RAW264.7ϒ NO^- Cells

To investigate the uptake of **DANPY-NO** by live cells, RAW264.7ϒ NO^- macrophages were incubated overnight with the probe and confocal LSM images were acquired showing bright green fluorescence upon excitation at 405 nm (**Fig. S14**). To further confirm that the observed green fluorescence was due to the **DANPY-NO** internalised by the macrophages, intracellular fluorescence emission spectra were recorded. The fluorescence emission spectrum of **DANPY-NO** inside RAW264.7ϒ NO^- matches that of **DANPY-NO** recorded in Dulbecco's Modified Eagle Medium (DMEM) cell culture medium (black and red, respectively, in Fig. 4a). Importantly, the fluorescence emission spectrum of untreated cells (green in Fig. 4a) did not exhibit the characteristic fluorescence emission band at *ca.* 520 nm typical of 1,8-naphthalimide derivatives.

To elucidate the localisation of **DANPY-NO** within the RAW264.7ϒ NO^- cells, colocalisation studies were performed using LysoTracker Red DND-99, a marker of acidic organelles. As it can be seen in Fig. 4b (see **Fig. S15** for scatterplot), there is a clear overlap between the fluorescence emission from **DANPY-NO** (green) and the fluorescence emission from the LysoTracker Red DND-99 (red), confirmed by the yellow spots visible when the green and the red channels are overlaid with the differential interference contrast (DIC) image. The degree of colocalisation between **DANPY-NO** and the LysoTracker in the acidic organelles was confirmed by a Pearson's correlation coefficient of 0.74 ± 0.02 ($n = 3$ images, *ca.* 20 cells), which is excellent considering that **DANPY-NO** does not have a pending specific targeting moiety like previously reported probes of this type [42–45].

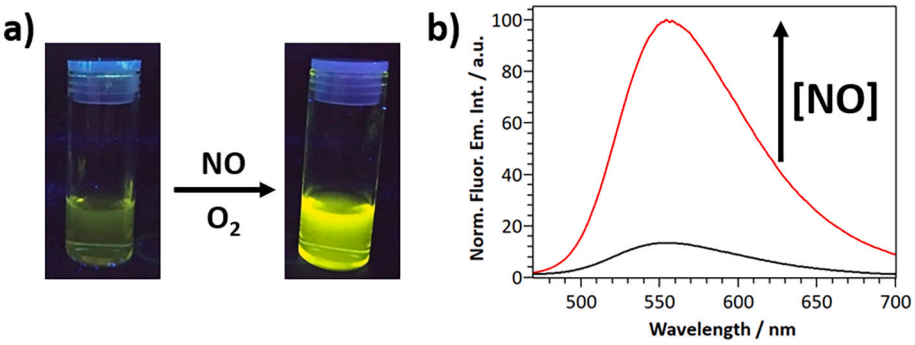

Fig. 2. NO detection using **DANPY-NO**: **a)** solutions containing **DANPY-NO** (62.5 μM in DMSO) under UV light, before (left) and after (right) addition of NONOate (3 mM); and **b)** fluorescence emission spectra of **DANPY-NO** (8.3 μM, aqueous solution, 13% DMSO) before (black) and after (red) addition of NONOate (0.5 mM). λ_{exc} = 396 nm. (For interpretation of the references to colour in this figure legend, the reader is referred to the web version of this article.)

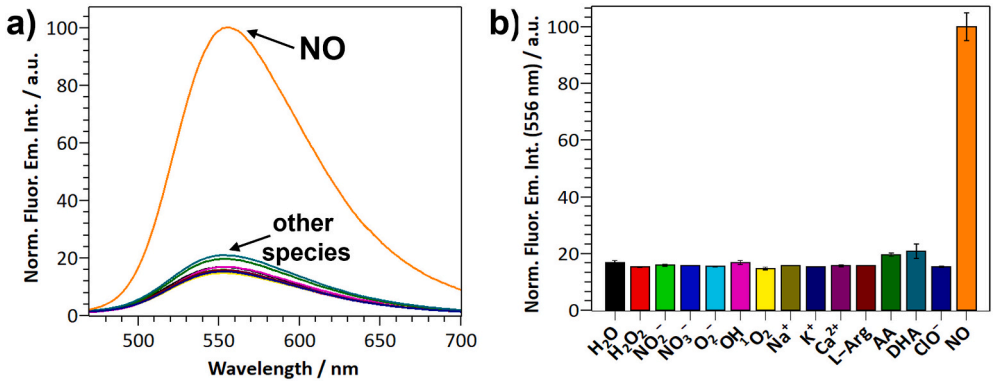

Fig. 3. Normalised **a)** fluorescence emission spectra and **b)** fluorescence response at 556 nm of **DANPY-NO** (8.5 μM) in the presence of NO and other biologically-relevant species (100 μM aqueous solution with 14% DMSO). λ_{exc} = 396 nm. Each experiment was repeated in triplicate and the relative standard errors are indicated by the error bars.

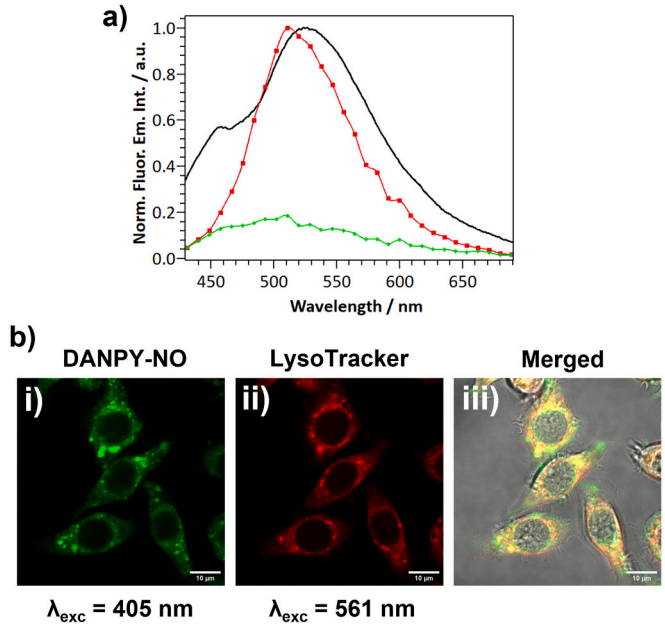

Fig. 4. a) Normalised fluorescence emission spectrum of: **DANPY-NO** in DMEM cell culture medium recorded in the fluorescence spectrophotometer (black); **DANPY-NO** internalised by RAW264.7ϒ NO^- cells recorded in the confocal LSM (red); and non-treated control cells recorded in the confocal LSM (green); λ_{exc} = 405 nm. **b)** Confocal LSM images of RAW264.7ϒ NO^- cells treated with **DANPY-NO** and LysoTracker Red DND-99. Images collected upon excitation at i) λ_{exc} = 405 nm, $\Delta\lambda_{em}$ = 500–580 nm and ii) λ_{exc} = 561 nm, $\Delta\lambda_{em}$ = 580–625 nm; and iii) composite image of green, red and DIC channels. Scale bars = 10 μm. (For interpretation of the references to colour in this figure legend, the reader is referred to the web version of this article.)

2.4. *Intracellular Application of **DANPY-NO** for the Detection of NO in Macrophages*

The potential of **DANPY-NO** to monitor NO concentrations in different cellular environments was investigated starting with its application in macrophages. The ability of **DANPY-NO** to detect endogenous NO was studied in RAW264.7ϒ NO^- macrophages stimulated overnight with lipopolysaccharide (LPS) and IFN-ϒ to produce elevated concentrations of NO. Following incubation, the cells were imaged using confocal LSM. Stimulated cells incubated with **DANPY-NO** exhibited higher green fluorescence emission intensity compared to those unstimulated cells incubated with the probe (Fig. 5). These results confirmed the successful detection of endogenous intracellular NO in

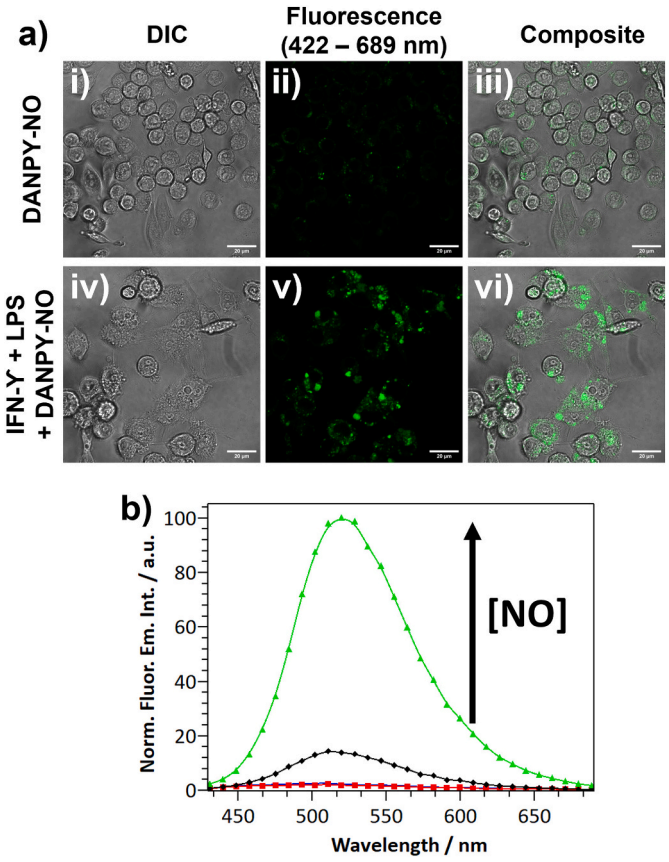

Fig. 5. a) Confocal LSM images and **b)** intracellularly recorded fluorescence emission spectra of RAW264.7ϒ NO^- cells incubated overnight with **DANPY-NO** (5 μM): unstimulated cells (i – iii images and black spectrum) and cells stimulated with LPS (0.7 μg/mL) and IFN-ϒ (17 μg/mL) (iv – vi images and green spectrum). Blue and red spectra correspond to untreated control cells stimulated and unstimulated, respectively. λ_{exc} = 405 nm; $\Delta\lambda_{em}$ = 422–689 nm. Scale bars = 20 μm. (For interpretation of the references to colour in this figure legend, the reader is referred to the web version of this article.)

live macrophages by **DANPY-NO**. It is also important to notice that non-treated cells, both stimulated and unstimulated, did not show any evident fluorescence emission (**Fig. S16**). To further confirm the enhancement of the fluorescence emission intensity of **DANPY-NO** in stimulated macrophages due to the formation of the triazole derivative, **DANPY-NO-T**, in the presence of NO, the intracellular fluorescence

emission spectra of the investigated samples were recorded. As expected, the fluorescence emission intensity in stimulated cells was higher compared to the intensity of unstimulated cells incubated with **DANPY-NO**; and negligible fluorescence was observed for unstimulated and stimulated control cells (Fig. 5b). Colocalisation experiments with LysoTracker Red DND-99 confirmed the overlap between the green fluorescence observed in stimulated cells incubated with **DANPY-NO** (fluorescence of **DANPY-NO-T**) and the red fluorescence of the marker of acidic organelles (Pearson's correlation coefficient of 0.71 ± 0.03 – n = 3 images, *ca.* 20 cells; **Fig. S17**). The successful performance of **DANPY-NO** in the detection of endogenous NO produced by stimulated RAW264.7ϒ NO^- cells was also confirmed by flow cytometry (**Fig. S18**). Cells stimulated with LPS and IFN-ϒ to produce NO and incubated with **DANPY-NO** exhibited a higher mean-fluorescence intensity compared to unstimulated cells incubated with **DANPY-NO**.

To prove the selective detection of NO by our probe, RAW264.7ϒ NO^- cells were treated with an inhibitor of the NOS, N(ω)-nitro-L-arginine methyl ester (L-NAME), to block the production of NO in stimulated RAW264.7ϒ NO^- cells, as confirmed with a Griess assay (**Fig. S19**). Cells pre-treated wtih L-NAME displayed a reduced fluorescence emission compared to the stimulated cells that did not receive a pre-treatment with L-NAME (**Fig. S20**) confirming the selectivity of **DANPY-NO** towards NO in RAW264.7ϒ NO^- cells.

An important feature to be considered when designing an intracellular fluorescent probe is the photobleaching of the probe over the irradiation time. To study the photostability of **DANPY-NO** over time, RAW264.7ϒ NO^- cells incubated with **DANPY-NO** were imaged at different exposure times following continuous irradiation (λ_{exc} = 405 nm). The photostability of our probe was compared to the photostability of DAF-2 DA (5 μM), a commercially available probe commonly used for the detection of intracellular NO (λ_{exc} = 488 nm). The fluorescence emission intensity of **DANPY-NO** exhibited a 16 ± 5% decrease after 5 min of continuous irradiation compared to a 38 ± 10% reduction observed for DAF-2 DA following the same irradiation time (Fig. 6 and **Fig. S21**). These results confirm the remarkable photostability of **DANPY-NO** which could be beneficial for long-term monitoring of biological processes involving NO generation, *e.g.* monitoring of NO released following bacterial infection.

Due to the excellent performance of **DANPY-NO** in sensing NO in RAW264.7ϒ NO^- macrophages, the next step was to evaluate its potential in primary mouse cells. Bone marrow-derived macrophages (BMDMs) were used as a model of primary cells. BMDMs were able to produce concentrations of nitrites of 30.4 ± 0.7 μM upon overnight stimulation with LPS (50 ng/mL) and INF-ϒ (100 ng/mL) compared to the negligible concentration of nitrites for unstimulated cells (0.6 ± 0.2 μM), as proven by the Griess assay. **DANPY-NO** was able to successfully detect NO endogenously produced by stimulated primary BMDMs (**Fig. S22**). Confocal LSM images of fixed cells stimulated and incubated with **DANPY-NO** exhibited higher fluorescence emission than the unstimulated cells incubated with **DANPY-NO** (**Fig. S22a**). BMDMs stimulated or unstimulated and without **DANPY-NO** loaded were also imaged as controls and exhibited no fluorescence. These results were further supported with the intracellular fluorescence emission spectra of the four different investigated samples, which clearly confirmed the ability of **DANPY-NO** to detect intracellular NO production in primary cells upon stimulation (**Fig. S22b**). Colocalisation experiments of **DANPY-NO** with LysoTracker Red confirmed the presence of the NO probe in the acidic organelles of the BMDMs (Pearson's correlation coefficient of 0.84 ± 0.10 – n = 3 images, *ca.* 10 cells; **Fig. S23**).

DANPY-NO was further evaluated in human macrophages, known to produce lower NO concentrations than previously investigated macrophages. THP-1 cells were selected for these experiments since they are acute monocytic leukemic cells derived from the peripheral blood of an infant. THP-1 cells were first differentiated to macrophages using phorbol 12-myristate 13-acetate (PMA) treatment overnight. The concentration of nitrites produced by the differentiated THP-1 cells upon stimulation with LPS (5 μg/mL) for 48 h was found to be 2.55 ± 0.07 μM using the Griess assay. Confocal LSM images of live PMA-differentiated THP-1 cells incubated with **DANPY-NO** and stimulated using LPS for 48 h exhibited a bright emission intensity that contrasted the weak fluorescence observed in the images of unstimulated cells incubated with **DANPY-NO** (**Fig. S24a**). This apparent fluorescence emission enhancement of **DANPY-NO** when detecting NO in human macrophages was further confirmed when the intracellular fluorescence emission spectra were recorded (**Fig. S24b**). Finally, the ability of **DANPY-NO** to specifically detect NO in THP-1 cells was investigated using L-NAME. Confocal LSM images of THP-1 cells pretreated with L-NAME exhibited intensities that were comparable to those observed for THP-1 cells unstimulated and incubated with **DANPY-NO**. As expected, the fluorescence emission spectrum of THP-1 cells treated with L-NAME, stimulated and incubated with **DANPY-NO** (red in **Fig. S24b**) overlapped the spectrum of unstimulated control cells incubated with **DANPY-NO** and that of unstimulated control cells treated with L-NAME and incubated with **DANPY-NO** (black and blue, respectively, in **Fig. S24b**). Control cells without **DANPY-NO** loaded (unstimulated cells and stimulated cells with and without L-NAME treatment) showed negligible fluorescence intensity in the corresponding confocal images (**Fig. S25**), which are supported by the corresponding intracellular fluorescence emission spectra. The presence of **DANPY-NO** within the acidic organelles of the PMA-differentiated THP-1 cells was confirmed by

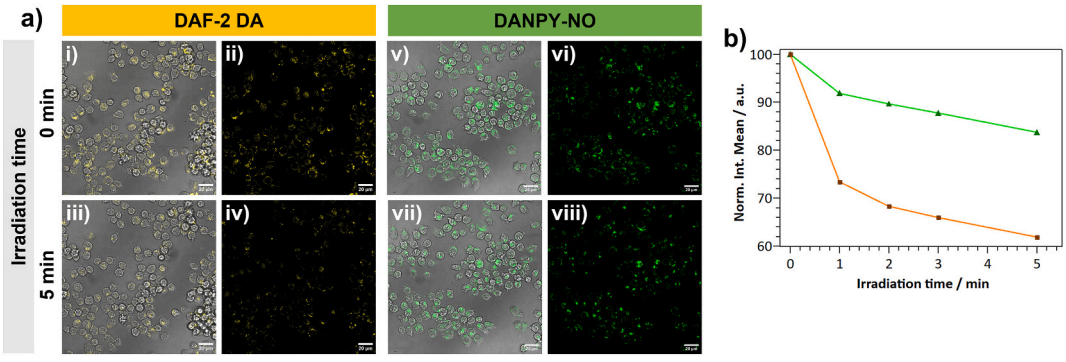

Fig. 6. a) Confocal LSM images of RAW264.7ϒ NO^- cells incubated with i – iv) DAF-2 DA (5 μM) or v – viii) **DANPY-NO** (5 μM), before (i, ii, v and vi) and following (iii, iv, vii and viii) 5 min laser irradiation (λ_{exc} (DAF-2 DA) = 488 nm/ $\Delta\lambda_{em}$ = 502–689 nm and λ_{exc} (**DANPY-NO**) = 405 nm/ $\Delta\lambda_{em}$ = 422–689 nm; laser power 5%). **b)** Normalised intensity mean values of images recorded with the confocal LSM at different irradiation time points of RAW264.7ϒ NO^- cells incubated with DAF-2 DA (orange) or **DANPY-NO** (green). Results are average values of three different experiments (three positions in three different cells). Intensity mean values obtained using ImageJ software. Scale bars = 20 μm. (For interpretation of the references to colour in this figure legend, the reader is referred to the web version of this article.)

colocalisation with LysoTracker Red (Pearson's correlation coefficient of 0.42 ± 0.06 – $n = 3$ images, *ca.* 10 cells; **Fig. S26**).

DANPY-NO was also able to monitor different concentrations of intracellular NO in THP-1 macrophages. Differentiated THP-1 macrophages were separately stimulated with two different concentrations of LPS (5 and 10 μg/mL). After overnight treatment, confocal LSM images and intracellular fluorescence emission spectra were recorded, which exhibited an increase in the fluorescence emission intensity of **DANPY-NO** concomitant with the increase in LPS concentration (Fig. 7; corresponding confocal LSM images shown in **Fig. S27**).

2.5. Intracellular Application of *DANPY-NO* for the Detection of NO in Endothelial Cells

To further explore the versatility of **DANPY-NO**, the potential of the probe to detect intracellular NO produced by eNOS was investigated in endothelial cells. NO is continuously produced by eNOS using L-arginine as substrate; and this production can be inhibited using L-NAME or enhanced by treating the cells with a Ca^{2+} ionophore, since eNOS is a Ca^{2+}-dependent enzyme. **DANPY-NO** was used to detect endogenous and exogenous NO in endothelial cells. To this aim, three types of samples containing **DANPY-NO** and their corresponding controls without the probe were prepared: 1) endothelial cells incubated with **DANPY-NO** overnight; 2) cells treated with Ca^{2+} ionophore A-23187 together with **DANPY-NO** overnight; 3) cells pre-treated with L-NAME and incubated with **DANPY-NO** overnight. As confirmed by the Griess assay, higher NO levels were produced by cells containing Ca^{2+} ionophore A-23187 (0.295 ± 0.004 μM) and lower NO concentrations were observed in cells pretreated with L-NAME (0.12 ± 0.02 μM), compared to untreated cells (0.21 ± 0.01 μM). The endothelial cells incubated with **DANPY-NO** and Ca^{2+} ionophore A-23187 showed an enhanced fluorescence emission intensity compared to those cells incubated only with **DANPY-NO** (**Fig. S28a**). In contrast, a reduction of the fluorescence emission intensity was observed for the cells pre-treated with L-NAME (**Fig. S28a**, vii – ix). Confocal LSM images of control samples showed negligible fluorescence emission (**Fig. S29**). These results were confirmed by the intracellular fluorescence emission spectra recorded also in the confocal LSM (**Fig. S28b**) which exhibited the same trend as the confocal LSM images. These results demonstrated the ability of **DANPY-NO** to monitor different endogenous NO levels in endothelial cells.

The ability of **DANPY-NO** to detect exogenous NO in endothelial cells was studied using *S*-nitroso-*N*-acetylpenicillamine (SNAP) as NO donor. Endothelial cells were incubated overnight with **DANPY-NO** in the presence and absence of SNAP (220 μM). Following the corresponding incubation, confocal LSM images and spectra were acquired (**Fig. S30**). The confocal images exhibited a small difference in fluorescence emissions between cells incubated with **DANPY-NO** and cells incubated with **DANPY-NO** and SNAP, the latter being the brightest and thus confirming the presence of higher concentrations of NO. These results were supported with the fluorescence emission spectra that showed a higher intensity for cells treated with SNAP compared to cells incubated only with **DANPY-NO**. The fluorescence emission spectra of control cells that were not incubated with **DANPY-NO** did not show the characteristic emission intensity of the compound. **DANPY-NO** was partially colocalised with LysoTracker Red (Pearson's correlation coefficient of 0.50 ± 0.10 – $n = 3$ images, *ca.* 5 cells; **Fig. S31**) in the endothelial cells.

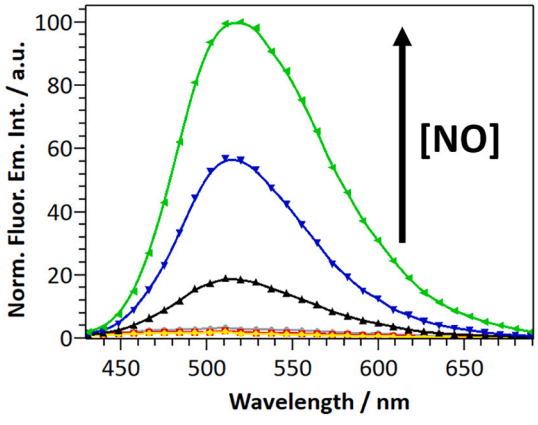

Fig. 7. Intracellularly recorded fluorescence emission spectra of THP-1 differentiated macrophages incubated with **DANPY-NO** (5 μM) and stimulated with different LPS concentrations (0, 5 and 10 μg/mL; black, blue and green spectra, respectively) overnight. Grey, red and yellow spectra correspond to cells without **DANPY-NO** and treated with 0, 5 and 10 μg/mL of LPS, respectively. λ_{exc} = 405 nm. (For interpretation of the references to colour in this figure legend, the reader is referred to the web version of this article.)

2.6. Intracellular Characterisation of *DANPY-NO* under Two-Photon Excitation

Given the excellent performance of **DANPY-NO** as NO probe in solution and under one-photon excitation (405 nm), the ability of **DANPY-NO** to be excited by two-photon excitation (800 nm), and to be used to monitor NO production under these conditions were investigated using a multiphoton microscope (Fig. 8). RAW264.7ϒ NO^- macrophages, unstimulated or stimulated with LPS and IFN-ϒ, were incubated with **DANPY-NO** overnight. After this time, live cells were imaged using 800 nm irradiation with fluorescence collected between 500 and 550 nm. Unstimulated cells incubated with **DANPY-NO** exhibited a green fluorescence emission (Fig. 8) that was not observed in the control cells which had not been incubated with **DANPY-NO** (**Fig. S32**). Additionally, stimulated cells incubated with **DANPY-NO** showed a remarkable enhancement of the green fluorescence (Fig. 8) as expected from the previous results using confocal LSM. These results confirmed the capacity of **DANPY-NO** to be visualised under NIR light (800 nm) and its potential to detect intracellular NO under two-photon excitation using multiphoton microscopy.

2.7. Cytotoxicity Experiments of *DANPY-NO*

Importantly, the cytotoxicity of **DANPY-NO** towards all the cellular systems used was determined by CellTiter-Blue viability assay showing a great biocompatibility in all the cases (**Fig. S33**). The cytotoxicity of

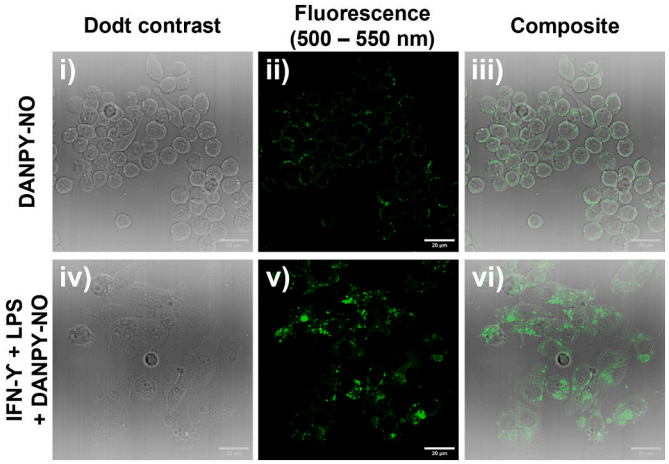

Fig. 8. Multiphoton microscopy images of RAW264.7ϒ NO^- cells incubated overnight with **DANPY-NO** (5 μM): unstimulated cells (i – iii) and cells stimulated with LPS (0.7 μg/mL) and IFN-ϒ (17 μg/mL) (iv – vi). λ_{exc} = 800 nm, $\Delta\lambda_{em}$ = 500–550 nm. Scale bars = 20 μm.

DANPY-NO towards RAW264.7ϒ NO^- macrophages showed a cell survival rate higher than 94% after overnight treatment with **DANPY-NO** (5 μM). In BMDMs, the cytotoxicity of **DANPY-NO** exhibited a cell viability of 88% when cells were incubated with the concentration of **DANPY-NO** used in the intracellular NO detection experiments (5 μM). Additionally, double the experimental concentration of **DANPY-NO** continued to exhibit low cytotoxicity to BMDMs. Cytotoxicity studies of **DANPY-NO** in PMA-differentiated THP-1 cells incubated for 48 h did not show a significant cell toxicity even at 10 μM (86% of cells were still viable). Finally, **DANPY-NO** also showed negligible cytotoxicity to endothelial cells in the range of concentrations used.

3. Conclusions

In summary, we have reported a highly versatile PET-based two-photon fluorescent probe, **DANPY-NO**, for the detection of NO produced by iNOS and eNOS in a wide selection of cells and at a different range of concentrations. In solution, **DANPY-NO** was selective to NO over other potential biological interferences, exhibited a LOD of 77.8 nM, suitable for the detection of endogenous NO produced by biological samples, and its fluorescence was stable at different, biologically-relevant, pH values. The versatility of **DANPY-NO** for the detection of intracellular NO was confirmed using a range of techniques including confocal LSM (images and intracellular fluorescence emission spectra), multiphoton microscopy and flow cytometry. The probe was successfully used for the selective detection of intracellular endogenous NO produced by iNOS and eNOS in a wide range of cells including: mouse macrophages, human leukemic cells, primary mouse macrophages and endothelial cells; demonstrating an excellent biocompatibility with all the listed cellular samples. Furthermore, **DANPY-NO** exhibited higher photostability than a frequently used commercially available NO probe. Overall, **DANPY-NO** has proven to be an excellent candidate for the monitoring of intracellular NO produced at low and high concentrations; and its two-photon excitation nature makes it potentially valuable for both *in vitro* and *in vivo* detection of NO.

Author Contributions

C. A. V performed all the experimental work described in this paper and analysed the data, wrote the original draft of the manuscript and the ESI and contributed to the later reviewing and editing. L. W. provided guidance on the synthesis of **DANPY-NO**. P. T. provided training and supervision of the imaging techniques and contributed to reviewing and editing the manuscript. R. J. contributed to the endothelial cell culture and provided help with the intracellular experiments involving endothelial cells. S. R. isolated and supplied the BMDMs, D. W. provided guidance on the endothelial work, contributed to reviewing and editing the manuscript. A. S. provided guidance on the BMDMs work and supplied the THP-1 cells. M. P. M. provided training and supervision of the synthesis of **DANPY-NO** and contributed to writing, reviewing and editing the manuscript. F. G. contributed to the design of the project and reviewing the manuscript. M. J. M. supervised the entire research with conceptualisation, analysis and re-sources, contributed to the writing, and coordinated the re-viewing and editing of the final manuscript. All authors have given approval to the final manuscript.

Declaration of Competing Interest

The authors declare that they have no known competing financial interests or personal relationships that could have appeared to influence the work reported in this paper.

Acknowledgment

The authors acknowledge Dr. A. Goldson for training and guidance on the flow cytometer; Dr. P. Wilson for training and guidance on the multiphoton microscope. The authors would like to thank the Faculty of Sciences and School of Chemistry at the University of East Anglia and Mr. and Mrs. Whittaker oncology fellowship for financial support, and the EPSRC (Grant EP/S017909/1) that supported the purchase of the Edinburgh Instrument FS5 fluorescence spectrometer used in this work.

Appendix A. Supplementary data

The SI contains the experimental section of this paper and the supporting figures including NMR spectra of **DANPY-NO** and its intermediates; electronic spectroscopic properties of **DANPY-NO** and sensitivity and selectivity characterisation; and supporting intracellular controls and further intracellular characterisation. Supplementary data to this article can be found online at https://doi.org/10.1016/j.jphotobiol.2022.112512.

References

[1] R.M.J. Palmer, A.G. Ferrige, S. Moncada, Nitric oxide release accounts for the biological activity of endothelium-derived relaxing factor, Nature 327 (1987) 524–526.
[2] A.R. Butler, D.L.H. Williams, The physiological role of nitric oxide, Chem. Soc. Rev. 22 (1993) 233–241.
[3] R.G. Knowles, S. Moncada, Nitric oxide synthases in mammals, Biochem. J. 298 (1994) 249–258.
[4] D.J. Stuehr, Mammalian nitric oxide synthases, Biochim. Biophys. Acta 1411 (1999) 217–230.
[5] S. Korde Choudhari, M. Chaudhary, S. Bagde, A.R. Gadbail, V. Joshi, Nitric oxide and cancer: a review, J. Surg. Oncol. 11 (2013) 118.
[6] C. Csonka, T. Páli, P. Bencsik, A. Görbe, P. Ferdinandy, T. Csont, Measurement of NO in biological samples, Br. J. Pharmacol. 172 (2015) 1620–1632.
[7] Y. Wang, D.C. Newton, P.A. Marsden, Neuronal NOS: gene structure, mRNA diversity, and functional relevance, Crit. Rev. Neurobiol. 13 (1999) 21–43.
[8] V. Calabrese, C. Mancuso, M. Calvani, E. Rizzarelli, D.A. Butterfield, A.M. Stella, Nitric oxide in the central nervous system: neuroprotection versus neurotoxicity, Nat. Rev. Neurosci. 8 (2007) 766–775.
[9] A.W. Deckel, Nitric oxide and nitric oxide synthase in Huntington's disease, J. Neurosci. Res. 64 (2001) 99–107.
[10] H. Li, U. Förstermann, Nitric oxide in the pathogenesis of vascular disease, J. Pathol. 190 (2000) 244–254.
[11] K.M. Naseem, The role of nitric oxide in cardiovascular diseases, Mol. Asp. Med. 26 (2005) 33–65.
[12] S.W. Norby, J.A. Weyhenmeyer, R.B. Clarkson, Stimulation and inhibition of nitric oxide production in macrophages and neural cells as observed by spin trapping, Free Radic. Biol. Med. 22 (1997) 1–9.
[13] W.J. Murphy, M. Muroi, C.Z. Zhang, T. Suzuki, S.W. Russell, Both basal and enhancer κB elements are required for full induction of the mouse inducible nitric oxide synthase gene, J. Endotoxin Res. 3 (1996) 381–393.
[14] D. Mishra, V. Patel, D. Banerjee, Nitric oxide and S-nitrosylation in cancers: emphasis on breast cancer, Breast Cancer 14 (2020), https://doi.org/10.1177/1178223419882688.
[15] A.B. Seabra, G.Z. Justo, P.S. Haddad, State of the art, challenges and perspectives in the design of nitric oxide-releasing polymeric nanomaterials for biomedical applications, Biotechnol. Adv. 33 (2015) 1370–1379.
[16] X. Zhang, G. Tian, W. Yin, L. Wang, X. Zheng, L. Yan, J. Li, H. Su, C. Chen, Z. Gu, Y. Zhao, Controllable generation of nitric oxide by near-infrared-sensitized upconversion nanoparticles for tumor therapy, Adv. Funct. Mater. 25 (2015) 3049–3056.
[17] M.T. Pelegrino, L.C. Silva, C.M. Watashi, P.S. Haddad, T. Rodrigues, A.B. Seabra, Nitric oxide-releasing nanoparticles: synthesis, characterization, and cytotoxicity to tumorigenic cells, J. Nanopart. Res. 19 (2017) 57.
[18] E. Eroglu, S. Charoensin, H. Bischof, J. Ramadani, B. Gottschalk, M.R. Depaoli, M. Waldeck-Weiermair, W.F. Graier, R. Malli, Genetic biosensors for imaging nitric oxide in single cells, Free Radic. Biol. Med. 128 (2018) 50–58.
[19] N.M. Iverson, E.M. Hofferber, J.A. Stapleton, Nitric oxide sensors for biological applications, Chemosensors 6 (2018) 8.
[20] E. Eroglu, S. Hallström, H. Bischof, M. Opelt, K. Schmidt, B. Mayer, M. Waldeck-Weiermair, W.F. Graier, R. Malli, Real-time visualization of distinct nitric oxide generation of nitric oxide synthase isoforms in single cells, Nitric Oxide 70 (2017) 59–67.
[21] L.H. Yang, D.J. Ahn, E. Koo, A "turn-on" fluorescent microbead sensor for detecting nitric oxide, Int. J. Nanomedicine 10 (2015) 115–123.
[22] E.M. Hetrick, M.H. Schoenfisch, Analytical chemistry of nitric oxide, Annu. Rev. Anal. Chem. 2 (2009) 409–433.
[23] H. Kojima, Y. Urano, K. Kikuchi, T. Higuchi, Y. Hirata, T. Nagano, Fluorescent indicators for imaging nitric oxide production, Angew. Chem. Int. Ed. 38 (1999) 3209–3212.
[24] H. Kojima, M. Hirotani, N. Nakatsubo, K. Kikuchi, Y. Urano, T. Higuchi, Y. Hirata, T. Nagano, Bioimaging of nitric oxide with fluorescent indicators based on the rhodamine chromophore, Anal. Chem. 73 (2001) 1967–1973.

[25] Y. Gabe, Y. Urano, K. Kikuchi, H. Kojima, T. Nagano, Highly sensitive fluorescence probes for nitric oxide based on boron dipyrromethene chromophore rational design of potentially useful bioimaging fluorescence probe, J. Am. Chem. Soc. 126 (2004) 3357–3367.
[26] E. Sasaki, H. Kojima, H. Nishimatsu, Y. Urano, K. Kikuchi, Y. Hirata, T. Nagano, Highly sensitive near-infrared fluorescent probes for nitric oxide and their application to isolated organs, J. Am. Chem. Soc. 127 (2005) 3684–3685.
[27] M.J. Marín, P. Thomas, V. Fabregat, S.V. Luis, D.A. Russell, F. Galindo, Fluorescence of 1,2-diaminoanthraquinone and its nitric oxide reaction product within macrophage cells, ChemBioChem 12 (2011) 2471–2477.
[28] H. Li, Y.-H. Hao, W. Feng, Q.-H. Song, Rapid and sensitive detection of nitric oxide by a BODIPY-based fluorescent probe in live cells: glutathione effects, J. Mater. Chem. B 8 (2020) 9785–9793.
[29] S. Ma, X. Sun, Q. Yu, R. Liu, Z. Lu, L. He, Dihydropyridine-coumarin-based fluorescent probe for imaging nitric oxide in living cells, Photochem. Photobiol. Sci. 19 (2020) 1230–1235.
[30] Q. Han, J. Liu, Q. Meng, Y.-L. Wang, H. Feng, Z. Zhang, Z.P. Xu, R. Zhang, Turn-on fluorescence probe for nitric oxide detection and bioimaging in live cells and zebrafish, ACS Sensors 4 (2019) 309–316.
[31] W.-L. Jiang, Y. Li, H.-W. Liu, D.-Y. Zhou, J. Ou-Yang, L. Yi, C.-Y. Li, A rhodamine-deoxylactam based fluorescent probe for fast and selective detection of nitric oxide in living cells, Talanta 197 (2019) 436–443.
[32] Y. Yu, X. Zhang, Y. Dong, X. Luo, X. Qian, Y. Yang, Fusing the Nagano's and the Anslyn's chemistry for lyso-specific NO detection, Sensors Actuators B Chem. 346 (2021), 130562.
[33] Y. Chen, Recent developments of fluorescent probes for detection and bioimaging of nitric oxide, Nitric Oxide 98 (2020) 1–19.
[34] L. Wang, J. Zhang, X. An, H. Duan, Recent progress on the organic and metal complex-based fluorescent probes for monitoring nitric oxide in living biological systems, Org. Biomol. Chem. 18 (2020) 1522–1549.
[35] D. Kim, H.G. Ryu, K.H. Ahn, Recent development of two-photon fluorescent probes for bioimaging, Org. Biomol. Chem. 12 (2014) 4550–4566.
[36] R.K.P. Benninger, D.W. Piston, Two-photon excitation microscopy for the study of living cells and tissues, Curr. Protoc. Cell Biol. (2013) 1–36.
[37] E.W. Seo, J.H. Han, C.H. Heo, J.H. Shin, H.M. Kim, B.R. Cho, A small-molecule two-photon probe for nitric oxide in living tissues, Chem. Eur. J. 18 (2012) 12388–12394.
[38] X. Dong, C.H. Heo, S. Chen, H.M. Kim, Z. Liu, Quinoline-based two-photon fluorescent probe for nitric oxide in live cells and tissues, Anal. Chem. 86 (2014) 308–311.
[39] Z. Mao, W. Feng, Z. Li, L. Zeng, W. Lv, Z. Liu, NIR in, far-red out: developing a two-photon fluorescent probe for tracking nitric oxide in deep tissue, Chem. Sci. 7 (2016) 5230–5235.
[40] M. Wang, Z. Xu, X. Wang, J. Cui, A fluorescent and colorimetric chemosensor for nitric oxide based on 1,8-naphthalimide, Dyes Pigments 96 (2013) 333–337.
[41] C.-B. Huang, J. Huang, L. Xu, A highly selective fluorescent probe for fast detection of nitric oxide in aqueous solution, RSC Adv. 5 (2015) 13307–13310.
[42] H. Yu, Y. Xiao, L. Jin, A lysosome-targetable and two-photon fluorescent probe for monitoring endogenous and exogenous nitric oxide in living cells, J. Am. Chem. Soc. 134 (2012) 17486–17489.
[43] W. Feng, Q.-L. Qiao, S. Leng, L. Miao, W.-T. Yin, L.-Q. Wang, Z.-C. Xu, A 1,8-naphthalimide-derived turn-on fluorescent probe for imaging lysosomal nitric oxide in living cells, Chin. Chem. Lett. 27 (2016) 1554–1558.
[44] N. Gupta, S. Imam Reja, V. Bhalla, M. Gupta, G. Kaur, M. Kumar, An approach for the selective detection of nitric oxide in biological systems: an in vitro and in vivo perspective, Chem. Asian J. 11 (2016) 1020–1027.
[45] S.-J. Li, D.-Y. Zhou, Y. Li, H.-W. Liu, P. Wu, J. Ou-Yang, W.-L. Jiang, C.-Y. Li, Efficient two-photon fluorescent probe for imaging of nitric oxide during endoplasmic reticulum stress, ACS Sensors 3 (2018) 2311–2319.
[46] A. Podder, M.M. Joseph, S. Biswas, S. Samanta, K.K. Maiti, S. Bhuniya, Amphiphilic fluorescent probe self-encored in plasma to detect pH fluctuations in cancer cell membranes, Chem. Commun. 57 (2021) 607–610.
[47] M.J. Marín, F. Galindo, P. Thomas, T. Wileman, D.A. Russell, A photoinduced electron transfer-based nanoprobe as a marker of acidic organelles in mammalian cells, Anal. Bioanal. Chem. 405 (2013) 6197–6207.
[48] M.J. Marín, F. Galindo, P. Thomas, D.A. Russell, Localized intracellular pH measurement using a ratiometric photoinduced electron-transfer-based Nanosensor, Angew. Chem. Int. Ed. 51 (2012) 9657–9661.
[49] S. Shamjith, M.M. Joseph, V.P. Murali, G.S. Remya, J.B. Nair, C.H. Suresh, K. K. Maiti, NADH-depletion triggered energy shutting with cyclometalated iridium (III) complex enabled bimodal luminescence-SERS sensing and photodynamic therapy, Biosens. Bioelectron. 204 (2022), 114087.
[50] H.W. Liu, S. Xu, P. Wang, X.X. Hu, J. Zhang, L. Yuan, X.B. Zhang, W. Tan, An efficient two-photon fluorescent probe for monitoring mitochondrial singlet oxygen in tissues during photodynamic therapy, Chem. Commun. 52 (2016) 12330–12333.